scientific reports

Check for updates

OPEN

Chronic rejection models for vascularized composite tissue allotransplantation

Daniel T. Fisher[1], Emily Mackey[2], Eugene Kononov[1], Paul N. Bogner[3], Umesh Sharma[4], Han Yu[5], Curtis L. Cetrulo[6], Mukund Seshadri[7], Pawel Kalinski[1], Joseph J. Skitzki[8], Elizabeth A. Repasky[1] & Minhyung Kim[1,2]✉

Vascularized composite tissue allotransplantation (VCA) has transformed patients' lives by enabling limb, face, abdominal wall, and penile transplants. Despite advancements in screening and immunosuppression, chronic rejection continues to limit the success of VCA. Lack of reliable preclinical models exacerbates this challenge. Here, we report on new mouse models of chronic rejection following heterotopic hind limb VCA. We employed different levels of MHC mismatch using CD8 knockout C57BL/6 mice as recipients along with BALB/c or B6 H2-Ab1^{bm12} mice as donors. Transient CD4 T cell depletion was induced to allow graft maturation. Evaluation included gross findings, changes in immune status changes, production of donor-specific antibodies (DSA), C4d levels, and histopathological alterations. Two chronic rejection models displayed common features of clinical chronic graft rejection, such as skin stricture, hair loss, adnexal atrophy, extensive fibrosis and mast cell infiltration without widespread necrotic changes common in acute rejection. Similar to chronic rejection patients, large populations of activated B and plasma cells were detected in the recipient's immune system as well as increased DSA and C4d production. Collectively, our models closely replicate the immunological and histopathological aspects of chronic graft rejection post-VCA, and could provide a new platform for evaluation of novel therapeutic interventions prior to clinical evaluation.

As advancements in modern medicine persistently improve survival rates among patients experiencing traumas resulting in limb loss or impairment of other functional units such as hands or faces, there is a growing impetus to expedite the healing process and empower these individuals to regain autonomy. Vascularized composite tissue allotransplantation (VCA) offers a pathway for carefully selected patients to reclaim functional replacements with the recovery of sensory and motor control following limb loss and facial disfigurement[1–7]. Nevertheless, owing to the necessity of utilizing transplants from deceased donors in VCA procedures, the donor pool remains limited and unpredictable. Consequently, unlike solid organ transplantation procedures such as kidney and lung transplants, the routine matching of human leukocyte antigen (HLA) between donor and recipient is not conducted[8]. Thus, there is a high rate of acute graft rejection (over 80%) as well as chronic graft rejection for hand and face transplantation[8]. Clinically, both acute and chronic rejection patterns are observed in VCA procedures. Acute rejection typically occurs during the immediate post-graft period, targeting primarily the skin and believed to be mostly T-cell mediated, as evidenced by cellular infiltrates identified in skin biopsies[9–11]. The immunology of chronic rejection is less well understood; however, it is associated with the development of graft vasculopathy that compromises blood flow to the graft, leading to loss of skin-associated tissue, atrophy of skin and muscles, and fibrosis[12]. Graft vasculopathy is initiated by anti-HLA donor-specific antibodies (DSA) binding to VCA endothelium, activating complement cascades which damage the endothelium, inducing myointimal proliferation and subsequent narrowing of the lumen[12–14].

Multiple preclinical animal models have been utilized to test novel approaches to prevent these rejection responses, resulting in significant improvements in the early phase of VCA graft survival[8,15,16]. However,

[1]Department of Immunology, Roswell Park Comprehensive Cancer Center, Buffalo, NY, USA. [2]Comparative Oncology Shared Resource, Roswell Park Comprehensive Cancer Center, Buffalo, NY, USA. [3]Department of Pathology, Roswell Park Comprehensive Cancer Center, Buffalo, NY, USA. [4]Department of Medicine, Division of Cardiology, University at Buffalo, Buffalo, NY, USA. [5]Department of Biostatistics and Bioinformatics, Roswell Park Comprehensive Cancer Center, Buffalo, NY, USA. [6]Department of Surgery, Division of Plastic Surgery, Cedars-Sinai Medical Center, Los Angeles, CA, USA. [7]Department of Oral Oncology, Roswell Park Comprehensive Cancer Center, Buffalo, NY, USA. [8]Department of General Surgery, Cleveland Clinic, Cleveland, OH, USA. ✉email: Minhyung.Kim@RoswellPark.org

these achievements are primarily limited to acute rejection responses acting through downregulation of T cell activation and proliferation. As the utilization of VCA surgery continues to rise and the management of acute rejection improves, chronic rejection is increasingly recognized as the primary obstacle to sustaining both the anatomical and functional integrity of VCA grafts[17]. Currently, there is no standard treatment to prevent the development of graft vasculopathy after VCA, and a reliable preclinical VCA model for chronic rejection responses is required to accelerate the development of novel treatment strategies.

There are many potential advantages to using a mouse model for VCA. Mouse major histocompatibility complex (MHC; H-2) is similar to the human MHC (HLA), and the mouse immune system is well-established. In addition, there is a wide array of gene knockout mouse models and a broad range of established mouse reagents, allowing for a more thorough investigation of chronic rejection mechanisms and the development of immunosuppression protocols after VCA. Preclinical animal models have been critical tools in improving scientific knowledge and human health, as well as providing new treatment strategies. Although a few research groups have used insufficient amounts of immunosuppressive drugs such as tacrolimus and cyclosporine to prolong VCA graft survival along with delayed graft rejection responses[18,19], this approach was based on T cell suppression, which is primarily related to acute rejection responses. Thus, the duration of graft survival was similar to chronic VCA rejection, but the mechanism of rejection was acute responses. Therefore, a novel preclinical chronic rejection model is required to investigate new treatment modalities. Here, we introduce novel and reliable chronic VCA rejection models that demonstrate characteristic histopathology and immune cell composition changes in the recipient.

Materials and methods

Mice

9–10 week-old aged female C57BL/6 J or B6.129S2-Cd8atm1Mak/J mice for recipients and C57BL/6 J (syngeneic [H-2^b]), BALB/c (allogeneic [H-2^d]), or B6(C)-H2-$Ab1^{bm12}$/KhEgJ (allogeneic [H2-$Ab1^{bm12}$]) mice for donors were purchased from the Jackson laboratory (Bar Harbor, ME). Mice were fed a standard laboratory diet and housed under standard light and accommodation conditions.

Peri-procedural care

Heterotopic cervical hind limb transplantations were performed by a single investigator (M.K.). All operations were carried out under sterile conditions, with animals kept on a heating surgical plate at 38 °C. Immediately before surgery, mice underwent anesthetic induction with 4% isoflurane inhalation (Abbott Laboratories, Chicago, IL) and maintained with 2% isoflurane inhalation via a nose cone. Puralube ophthalmic ointment (Dechra Veterinary Products, Overland Park, KS) was applied for eye protection. Donors were euthanized after harvesting the left hindlimb. All recipient mice were recovered on a warm water circulating blanket, injected subcutaneously with Ethiqa XR (3.25 mg/kg body weight) for pain control, and given saline (0.5 mL) subcutaneously to prevent dehydration. All experimental protocols were approved by the Roswell Park Comprehensive Cancer Center Institutional Animal Care and Use Committee.

VCA surgery

The surgery was carried out as described in our previous published work[20,21]. Briefly, a donor's common iliac and femoral vein were used for revascularization with a recipient's common carotid artery and external jugular vein respectively using a non-suture cuff technique. We used C57BL/6 background strain as recipients due to BALB/c strains having a higher anatomic variability inthe Circle of Willis than C57BL/6 strain and associated potential risk of cerebral ischemia[20].

Drug treatment

Immunosuppression was induced in mice using tacrolimus (Sigma-Aldrich, St. Louis, MO) in doses of 2.25 mg/kg (in DMSO; Sigma-Aldrich, St. Louis, MO) injected subcutaneously with a micro syringe (Hamilton, Reno, NV) daily. The 15 µg/µL of tacrolimus concentration was prepared, and 3 µL of diluent was injected without notable toxicity.

CD4 T cell depletion

InVivoMAb anti-mouse CD4 antibody (clone GK1.5) from BioXcell (Lebanon, NH) was used to deplete CD4 T cells transiently. 200 µg of the antibody was injected intraperitoneally in recipients 3 times, 2 days before VCA, the day of VCA, and 2 days after VCA.

Hematoxylin & Eosin (H&E), Trichrome, and immuno histo chemical (IHC) staining

Following standard euthanasia, grafted tissue was harvested and immersion fixed in 10% neutral-buffered formalin for 2 days (Thermo Scientific, Waltham, MA). The tissues were routinely processed and embedded in paraffin. Formalin fixed paraffin sections were sectioned at 4 µm, placed on charged slides, and dried at 60 °C for one hour. Slides were deparaffinized with Bond Dewax Solution (Leica, Allendale, NJ) and rinsed in water. H&E (Leica, Allendale, NJ) and trichrome (Poly Scientific R&D, Bay Shore, NY) stains were performed per manufacturers' instruction. For IHC, the slides were blocked using peroxide block from Bond Polymer Refine Detection kit (Leica, Allendale, NJ) for 5 min, and then the slides were incubated with B220 Antibody (BD Biosciences, San Jose, CA) at 1/100 for 20 min followed by Rabbit Envision (Agilent Technologies, Santa Clara, CA) for 30 min. Diaminobenzidine from the Bond Polymer Refine Detection kit (Leica, Allendale, NJ) was applied for 10 min for visualization.

Assessment of rejection grade

Gross pathology rejection grades were evaluated by M.K. based on the Banff 2022 working classification of skin-containing composite tissue allograft pathology[22]. Blinded to treatment group, post hoc histopathological scoring was performed by board-certified veterinary and clinical pathologists (E. M. and P.N.B.), respectively. Tissues were scored using a previously published scoring scheme for skin-containing vascularized composite allografts[23] and the Banff 2022 rejection grades[24]. The Banff Classification provides a standardized framework for assessing rejection in VCA, particularly focusing on skin-containing grafts. It categorizes rejection severity from Grade 0 (No Rejection), characterized by the absence or rarity of inflammatory cells, to Grade 4 (Necrotizing Acute Rejection), marked by extensive tissue necrosis. Intermediate grades include Grade 1 (Mild Rejection) with mild perivascular inflammation, Grade 2 (Moderate Rejection) with moderate-to-severe perivascular inflammation and limited epidermal involvement, and Grade 3 (Severe Rejection) featuring dense inflammation with significant epidermal damage, including apoptosis and dyskeratosis. This classification has undergone revisions to enhance the precision of rejection assessment in VCA, particularly concerning vascular involvement in 2022. In addition, adnexal atrophy, dermal fibrosis, and increased mast cell presence in the dermis were assessed based on a severity scale of 0 to 4. Histopathological rejection grades were evaluated in VCA grafts at 1-, 2-, and 6-weeks post-transplantation for the acute, chronic KO, and chronic BM12 grafts, respectively, while syngeneic grafts were assessed at 4 weeks following VCA. In the chronic rejection models utilizing a low dose of tacrolimus, transplanted grafts were assessed at 2 weeks in the chronic KO model and at 6 weeks in the chronic BM12 model following VCA.

Flow cytometry

The blood, bone marrow (BM) and spleen were collected at week 4 for the syngeneic, week 1 for the acute, week 2 for the chronic KO, and week 6 for the chronic BM12 rejection models after VCA. Blood was collected from the right superficial temporal vein (STV) using a sterile 5-mm animal lancet (Medipoint, INC., Mineola, NY) into K_3 EDTA coated tube (BD Bioscience, San Jose, CA) after anesthesia induction. The bone marrow (BM) cells were isolated from the recipient's left femur as described previously[25]. Spleens were mechanically disrupted and directly passed through a 70 µm nylon cell strainer (Alkali Scientific, Pompano Beach, FL). Red blood cells in each sample were depleted by hypotonic lysis buffer (Gibco, Gaithersburg, MD). Prepared cells were stained with different antibodies for extracellular markers. Antibodies of CD45 (BUV395, clone; 30-F11), CD3 (Alexa Fluor 700, clone; 17 A2), CD4 (PerCp, clone; RM4.5), CD8 (Alexa Fluor 488, clone; 53–6.7), CD19 (BB515, clone; 1D3), CD45R (PE-CF594, clone; RA3-6B2), MHC I-A (BV711, clone; M5/114), CD138 (APC, clone; 281–2), Ig G (FITC, clone; Poly4060), and Ig M (APC, clone; II/41) were used (BD Bioscience, San Jose, CA). All data were collected on an LSR Fortessa flow cytometer (BD Biosciences, San Jose, CA) and analyzed with WinList 9.0 software (Verity Software House, Topsham, ME).

ELISA

Mouse complement fragment 4 d (C4 d) ELISA kit was purchased from MyBioSource (San Diego, CA), and plasma was used to quantify levels of C4 d per the manufacturer's instructions. Plasma was collected from blood in K_3 EDTA coated tubes centrifuged for 20 min at 1000 × g at 5 °C within 1 h of blood collection. The plasma was kept at −80 °C until performing ELISA. 100µL of plasma was added in each well without dilution for analysis.

A rapid ex-vivo cell incubation

The rapid *ex-vivo* cell incubation was performed in 96-well U-bottom microtiter plates (Alkali Scientific, Fort Lauderdale, FL). 2×10^6 leukocytes from a donor's spleen were cocultured with 100µL of plasma from a VCA recipient at 37 °C for 1 h, and then the isolated cells were stained with antibodies for flow cytometry analysis.

Statistical analysis

All experiments were conducted in three independent replicates, and pooled data are presented. The ELISA study was performed three times, with representative results used for statistical analysis. Comparison between groups were performed using Student's t test, and statistical significance was accepted with *; $p < 0.05$, **; $p < 0.01$, and ***; $p < 0.001$. Log-rank (Mantel-Cox) test was used for survival comparisons between groups using GraphPad Prism, Version 8 software (GraphPad Software, Inc., La Jolla, CA).

Ethics declarations

All methods were carried out in accordance with relevant guidelines and regulations including ARRIVE guidelines. The experimental animals were euthanized under deep plane anesthesia, followed by exsanguination via cervical dislocation.

Results

Impact of donor and recipient strains on graft survivals

As clinical data and our previous work with acute rejection models of VCA suggested a central role for CD8 T cells mediating the large tissue necrosis[21,26], the elimination of anti-graft CD8 T cells was essential for the development of a chronic rejection model. Thus, four different groups of VCA were generated as a syngeneic control, an acute, and two chronic allogeneic rejection models. C57BL/6 J mice were used for both donors and recipients in the syngeneic model. For the acute rejection model, a total MHC mismatch transplant was performed between BALB/c and C57BL/6 J strains. Two different chronic rejection models were set after VCA between BALB/c donors and B6 CD8 KO recipients (*i.e.,* Chronic KO), and between B6 BM12 donors and B6 CD8 KO recipients (*i.e.,* Chronic BM12). No immunosuppressive drug was used before or after VCA to establish the most aggressive acute or chronic rejection models, and anti-mouse CD4 ab was injected in the two chronic

rejection models. There was no evidence of gross rejection 50 days after VCA in the syngeneic group. In the acute rejection group, all recipient mice showed grade 4 rejection within 8 days. No recipient mice showed any signs of rejection such as visual skin color change, desquamation, or skin crusting within 12 days after VCA in the chronic KO rejection group. The median survival was 14 days in the chronic KO rejection group and was significantly longer than 7 days seen in the acute rejection group. About 17% of the chronic BM12 recipients showed signs of gross rejection 4 weeks after VCA, and over 65% of the transplanted grafts did not reveal any gross rejection signs until 7 weeks after VCA. These two chronic rejection models prolonged the graft survival significantly compared to acute rejection recipients with graft survival maintained significantly longer in the chronic BM12 recipients compared to the chronic KO recipients (Fig. 1).

B and T cell compositions in the bone marrow and spleen after VCA

In the setting of total MHC mismatch and MHC disparity in an acute and both chronic rejection groups significant increases in B cell populations in bone marrow and spleen were noted as compared to the syngeneic group (Fig. 2A). Even though there is no increase of the B cell population between the acute and chronic rejection groups in the BM, significantly more B cells were detected in the spleen from the chronic rejection groups compared to the acute rejection group (Fig. 2A). In addition, these cells were identified as activated B cells ($B220^+CD19^+$MHC class II^+CD138^-) and plasma cells ($B220^+CD19^+$MHC class II^+CD138^+) (Fig. 2A) which can drive antigen presentation and further immune activation and may be undergoing activation and proliferation in response to chronic VCA rejection[27,28]. Significantly large amounts of activated B cells in the spleen and plasma cells in the BM were found in both chronic rejection models compared to the acute rejection group. Hence, a significant increase in the plasma cell population was detected in the chronic BM12 group compared to the chronic KO group in the BM (Fig. 2A). CD8 T cell populations in the acute rejection group increased significantly both in the BM and spleen compared to the syngeneic model (Fig. 2B) with the CD8 KO mice recipients in the chronic rejection groups demonstrating minimal levels of CD8 cells in the BM and spleen. CD4 T cell populations were lower in the chronic KO rejection group compared to the syngeneic group in the spleen with significantly larger compositions of CD4 T cell populations in the BM and spleen detected in the chronic BM12 group compared to other groups (Fig. 2B). CD4 T cell subsets central memory (CM) ($CD44^+CD62L^+$) and effector memory (EM) ($CD44^+CD62L^-$) were analyzed. Significant increases in the compositions of EM cells in the chronic KO rejection group were detected both in the BM and spleen compared to the other groups, and larger composition of the CM population was detected in the spleen (Fig. 2C). Furthermore, larger compositions of CD4 CM and EM populations in the BM were detected in the chronic BM12 group compared to the syngeneic group, but there was no significant difference in these populations between the acute and chronic BM12 groups (Fig. 2C).

Levels of donor specific antibodies and circulating C4 d in VCA recipients

A rapid *ex-vivo* cell incubation was performed to analyze levels of DSA in recipients' plasma with donor's splenocytes after different settings of VCA. Significantly more IgG^+ cells were detected after the incubation in the acute and two chronic rejection models compared to the syngeneic model, furthermore significant more amounts of IgG positive cells were detected in the chronic VCA recipients than the acute VCA recipients (Fig. 3A). The chronic BM12 model had the highest levels of IgG^+ cells. In addition, C4 d levels were measured in recipients' plasma by ELISA when the transplanted grafts showed over grade 3 gross rejection signs (the syngeneic recipients were euthanized 14 days after VCA without any rejection evidence). While the levels of C4

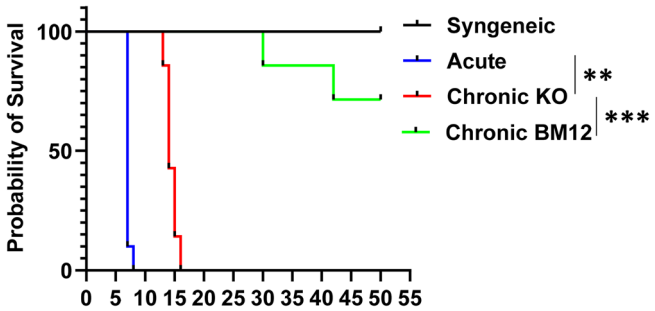

Fig. 1. Graft survival curves after vascularized composite tissue allotransplantation (VCA) in the syngeneic, acute, chronic KO, and chronic BM12 rejection models. C57BL/6 mice were used as donors and recipients in the syngeneic model, and BALC/c strain was used as a donor for the acute and chronic KO rejection models with different strains for recipients as C57BL/6 WT and C57BL/6 CD8 KO respectively. In the chronic BM12 model, B6(C)-H2-$Ab1^{bm12}$ donors were transplanted to C57BL/6 CD8 KO recipients. VCA was performed at Day 0, and the gross finding was assessed every day. The survival of the syngeneic group was significantly prolonged compared to the acute and chronic KO rejection groups (***$P < 0.001$), and the grafts in the chronic rejection groups showed significantly delayed rejection responses compared to the acute rejection group (chronic KO; **$P < 0.01$, chronic BM12; **$P < 0.001$). In addition, the chronic BM12 group showed significant rejection delay compared to the chronic KO group. Pooled data from 3 independent experiments. *Syngeneic; n = 5, acute; n = 10, chronic KO; n = 7, and chronic BM12; n = 9.*, ****$P < 0.0001$ by Log-rank test with GraphPad Prism.

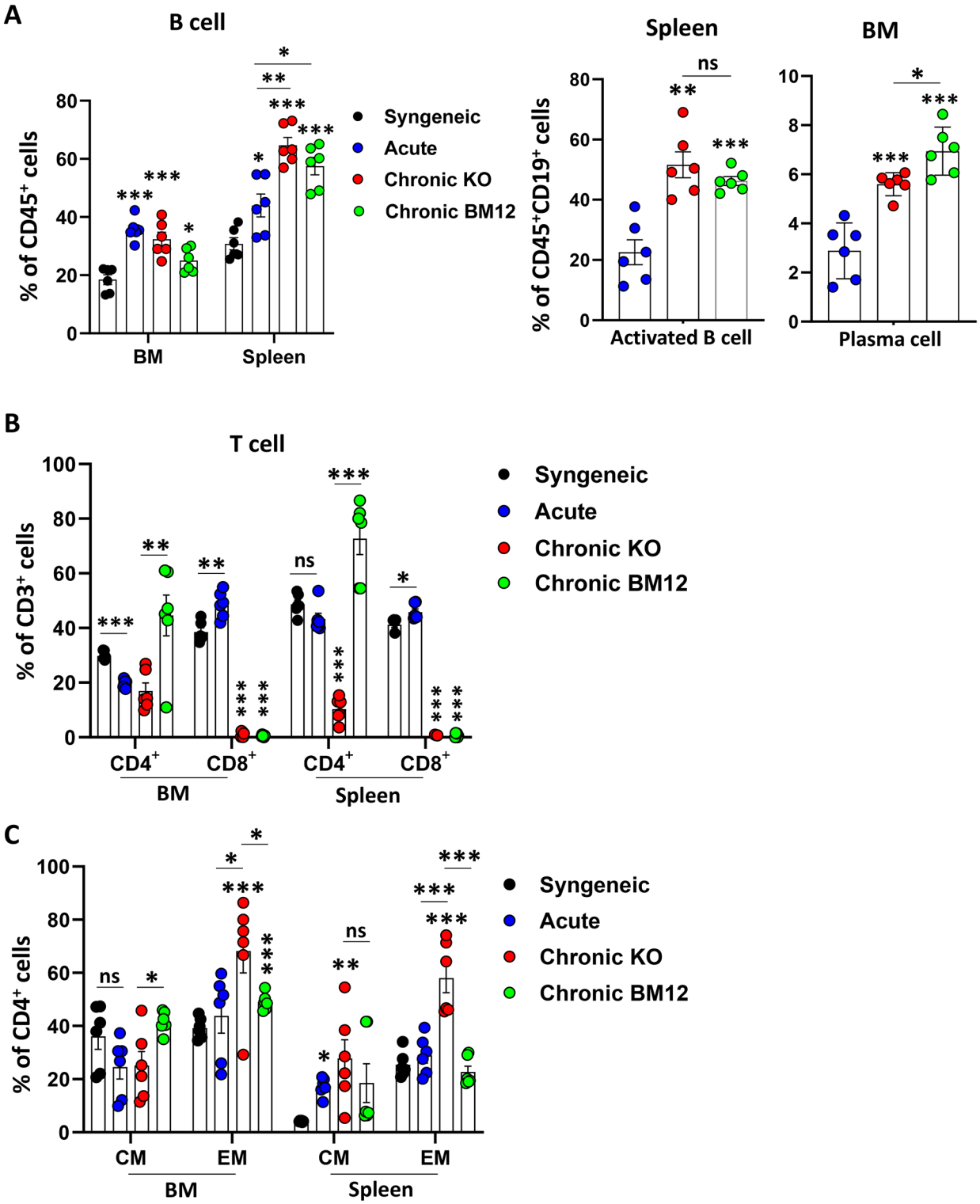

Fig. 2. Analysis of immune cell populations after VCA in the context of acute and chronic rejection. Activated B cells, plasma cells, and CD4 effector memory T cells increase significantly in the chronic rejection models. **A**, The composition of B cell population ($CD45^+CD3^-B220^+$) was analyzed in the BM and spleen at week 4 for the syngeneic, at week 1 for the acute, at week 2 for the chronic KO, and at week 6 for the chronic BM12 rejection model after VCA. And activated B cell ($CD45^+CD3^-B220^+CD19^+MHC\ II^+CD138^-$) and plasma cell ($CD45^+CD3^-B220^+CD19^+MHC\ II^+CD138^+$) were analyzed in the spleen and BM respectively. **B**, The compositions of CD4 and CD8 T cell populations were investigated in the BM and spleen under different settings. **C**, CD4 T cells were subclassified depending on the status of CD44 and CD62L positivity such as central memory (CM; $CD44^+CD62L^+$) and effector memory (EM; $CD44^+CD62L^-$) in the BM and spleen. Pooled data from 3 independent experiments. $n = 6$, ns; not significant, $^*P < 0.05$, $^{**}P < 0.01$, $^{***}P < 0.001$ by Student's t test, error bar; standard error of the mean.

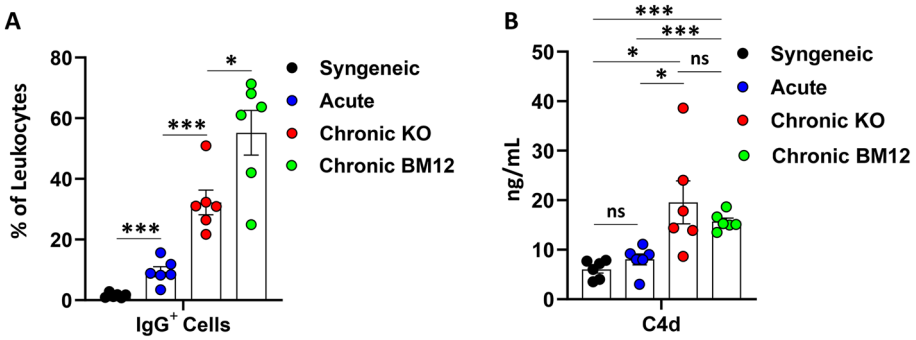

Fig. 3. Increases in the levels of donor specific antigen (DSA) and C4 d in the systemic circulation of chronic rejection model recipients. **A**, A rapid *ex-vivo* incubation was performed between a donor's (BALB/c or C57BL/6 backgrounds) lymphocytes and a recipient's plasma. The plasma was collected after 4 weeks for the syngeneic, 1 week for acute, 2 weeks for chronic KO, and 6 weeks for chronic BM12 rejection groups after VCA. After 1 h incubation at 37 °C, Ig G^+ cells on lymphocytes were analyzed by flow cytometry. $n = 6$, $^{***}P < 0.001$ by Student's t test, error bar; standard error of the mean. **B**, C4 d levels were measured by ELISA using recipients' plasma. Representative data from 3 independent experiments. $n = 6$, ns; not significant, $^{*}P < 0.05$ by Student's t test, error bar; standard error of the mean.

d in plasma did not show any statistical differences between the syngeneic and acute rejection models, significant increases in the circulating C4 d levels were detected in two chronic rejection models compared to the syngeneic and acute rejected recipients, but no significant difference was detected in the C4 d levels between two chronic rejection models (Fig. 3B).

Gross and histological evaluation of VCA rejection

While the syngeneic model showed normal hair growth on the graft (Fig. 4A), distinct manifestations of gross rejection varied in the acute and chronic rejection groups. The graft of acute rejection model revealed necrotic skin color change to black in the entire transplanted skin (Fig. 4B). The graft in the chronic KO recipients showed rough and scaly contracted skin with general hair loss (Fig. 4C) while the chronic B12 recipients exhibited hair loss and dry skin (Fig. 4D).

Histopathological rejection grades were assessed in the VCA grafts. Histology revealed mononuclear cell infiltration in the dermis and epidermis of the transplanted grafts that was more severe in the acute rejection model (Fig. 4F, 5A-D) compared to the grafts from the syngeneic (Fig. 4E and 5A-D) or chronic models (Fig. 4G-H and 5A-D). The degree of inflammation correlated with the defined BANFF grading schema, and also demonstrated that the acute rejection model had a greater degree of epidermal involvement characterized by epithelial apoptosis and dyskeratosis (Grade III) compared to all other groups (Fig. 5E). Features of chronic rejection in the skin including adnexal atrophy, dermal fibrosis, and increased mast cell presence in the dermis, were observed more frequently and with greater severity in the chronic rejection models (Fig. 5F-H). These findings were particularly pronounced in the chronic BM12 recipients (Fig. 4H and 5F-G). In addition, a significant number of mast cells were observed in both chronic rejection models, whereas none were detected in the syngeneic or acute rejection grafts (Fig. 4G-H and 5H).

The extent of fibrosis within the transplanted tissue was visualized and assessed using trichrome staining (Fig. 6). The stain highlights collagen fibers, which are characteristic of fibrotic tissue as a marker of chronic rejection responses. In correlation with the H&E findings, there was increased collagen deposition throughout the dermis of the grafts in the chronic rejection models compared to the acute rejected- and syngeneic transplanted grafts (Fig. 6A-D). Further, there was increased collagen deposition in patchy areas in the subcutis and throughout the fascial layers of the muscle in the grafts from the chronic rejection models (Fig. 6C-D). Interestingly, there was more fibrosis in the skin and deeper tissue of the syngeneic graft than the acutely rejected graft (Fig. 6A-B).

Chronic allograft vasculopathy (CAV) plays a central role in chronic rejection, the leading cause of long-term graft failure across various types of transplants including VCA[29]. CAV in arteries is defined by persistent intimal hyperplasia, vascular narrowing, and intimal arteritis[13]. The presence of CAV was evaluated, and the majority of chronically rejected grafts exhibited characteristics consistent with CAV (Fig. 7). Even though all syngeneic grafts showed significant intimal thickening (Fig. 7A), intimal arteritis was not prominent in this group (Fig. 7B). While intimal thickening is an important feature of CAV, it is not sufficient for diagnosis unless accompanied by immune-mediated injury, arteritis[30]. In contrast, mononuclear cell infiltration beneath the arterial endothelium and fibrinoid necrosis of the arterial wall were more evident in the chronic rejection groups along with significant intimal thickening (Fig. 7A). The majority of chronic KO recipients (3 out of 4) exhibited arteritis with intimal thickening. Notably, three additional recipients, despite lacking a large artery for analysis, demonstrated severe arteritis and intimal thickening in small arteries. Similarly, in chronic BM12 recipients, 5 out of 7 presented with concurrent intimal arteritis and thickening, while two recipients were excluded due to the absence of a large artery for evaluation (Fig. 7B).

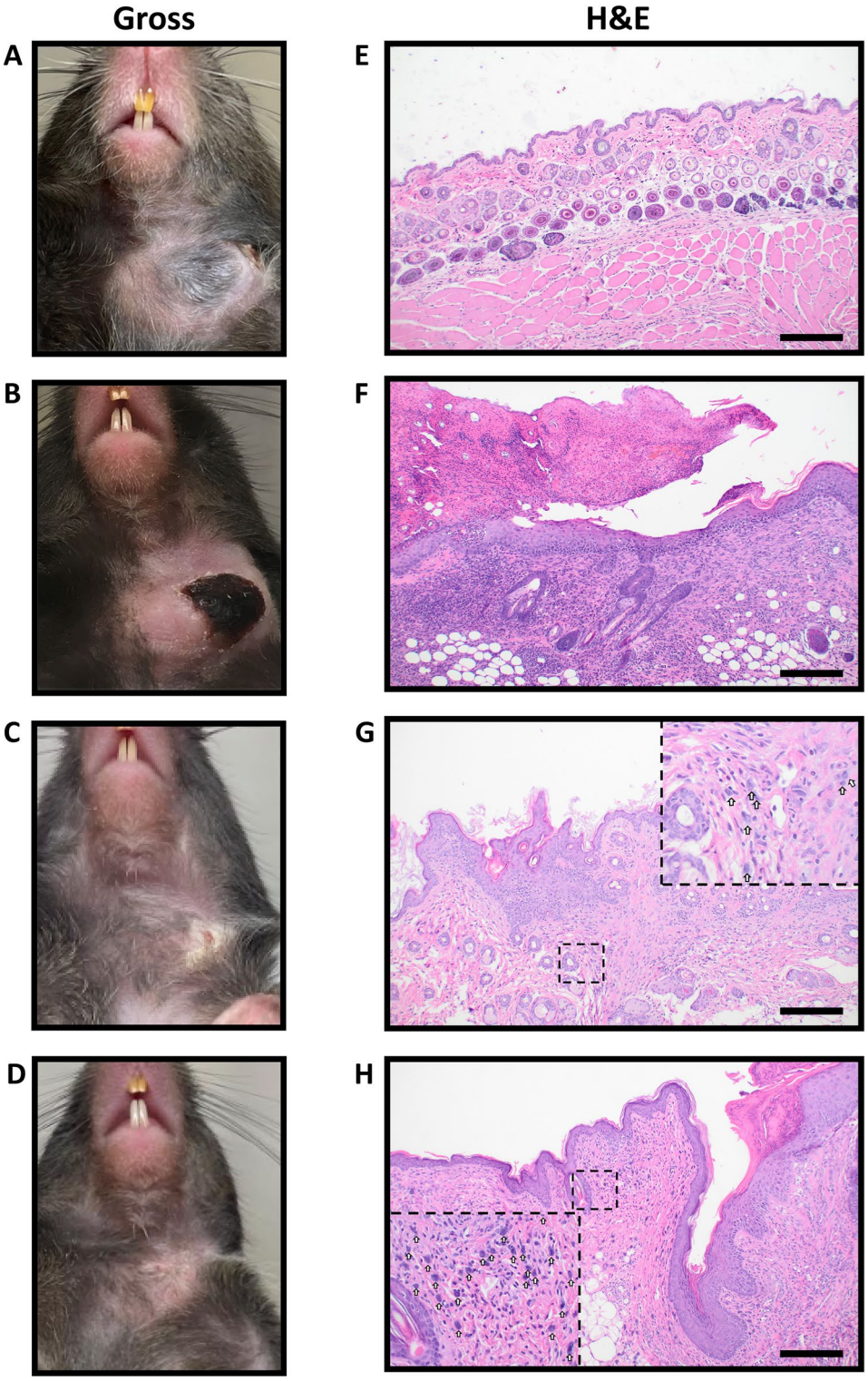

Fig. 4. Representative gross and histologic changes in mice after VCA. **A**, Gross image of a syngeneic recipient's graft 4 weeks after VCA. **B**, Gross image of an acutely rejected recipient's graft 1 week after VCA. **C**, Gross image of a chronic KO rejected recipient's graft 2 weeks after VCA. **D**, Gross image of a chronic BM12 rejected recipient's graft 6 weeks after VCA. **E**, H&E-stained image of a skin section from syngeneic recipient 4 weeks after VCA. Scale bar; 100 μm. **F**, H&E-stained image of a skin section from acute rejection recipient 1 week after VCA. Scale bar; 100 μm. **G**, H&E-stained image of a skin section from chronic KO recipient 2 weeks after VCA. Scale bar; 100 μm. **H**, H&E-stained image of a skin section from chronic BM12 recipient 6 weeks after VCA. Arrows; mast cell, scale bar; 100 μm.

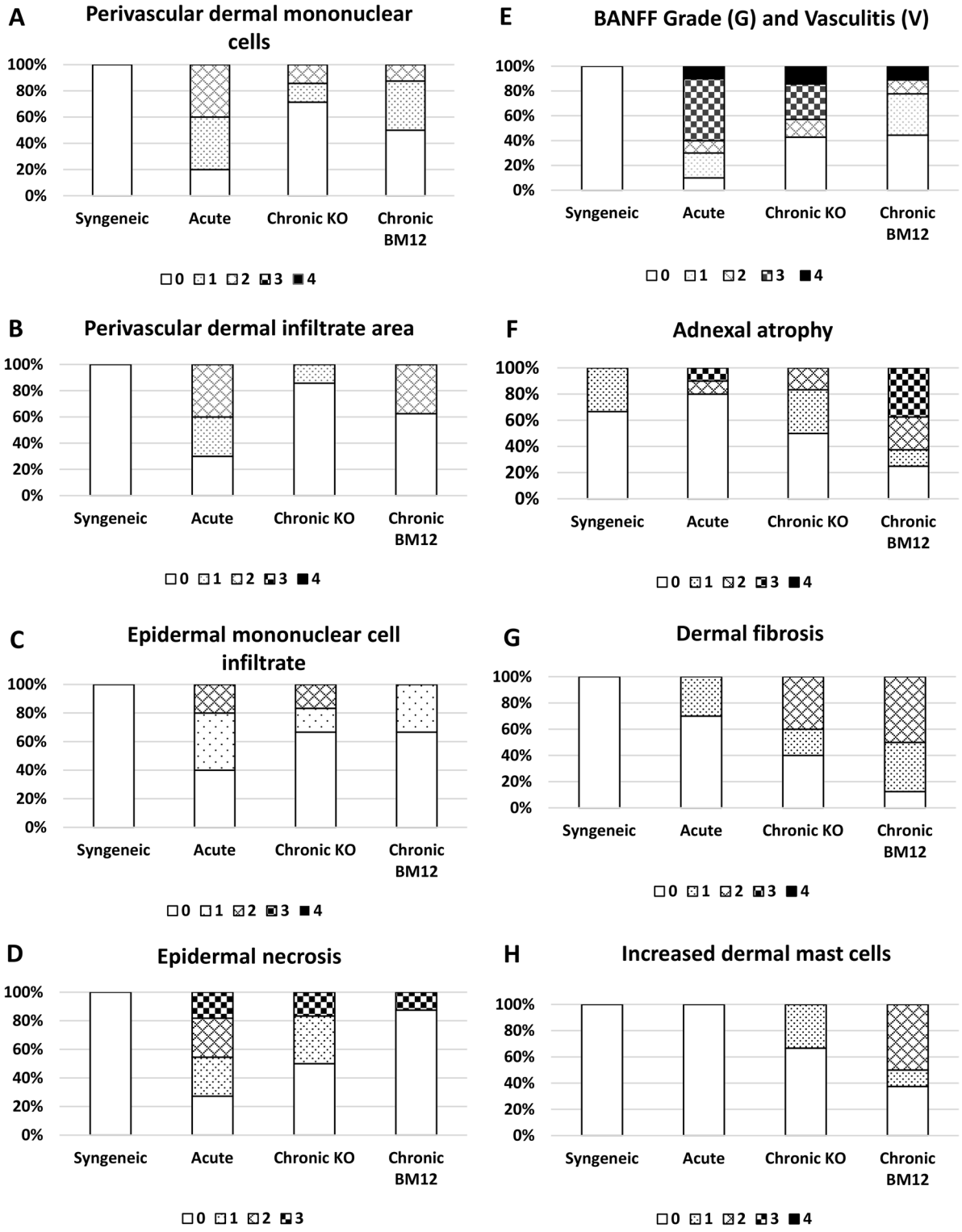

Fig. 5. Histopathological scores of the transplanted grafts. **A**. Stacked column graph of perivascular mononuclear cell infiltration in the superficial and deep dermis (0; < 10cells/vessel, 1; 10–25 cells/vessel, 2; 26–50 cells/vessel, 3; > 50cells/vessel). **B**, Stacked column graph of perivascular mononuclear cell dermal infiltrate area expressed as percent area occupied by the most involved dermal vessels at 40 × (0; < 25%, 1; 25–50%, 2; 50–75%, 3; > 75%). **C**, Stacked column graph of mononuclear cell infiltrate into epidermis (0; < 10 cells per 4, 20 × fields, 1; 10–20 cells per 4, 20 × fields, 2; > 20 cells per 4, 20 × fields, and 3; transdermal infiltrate). **D**, Stacked column graph of epidermal necrosis as presence of keratinocyte apoptosis and necrosis (0; none, 1; apoptosis, 2; focal necrosis, 3; sloughed). **E**, Stacked column graph of BANFF rejection scores. **F**, **G**, and **H**, Stacked column graph of adnexal atrophy, dermal fibrosis, and mast cell counts in the dermis, respectively (0; none, 1; minimal, 2; mild, 3; moderate, 4; severe). Pooled data from 3 independent experiments. Syngeneic; $n = 3$, acute; $n = 10$, chronic KO; $n = 7$, and chronic BM12; $n = 9$.

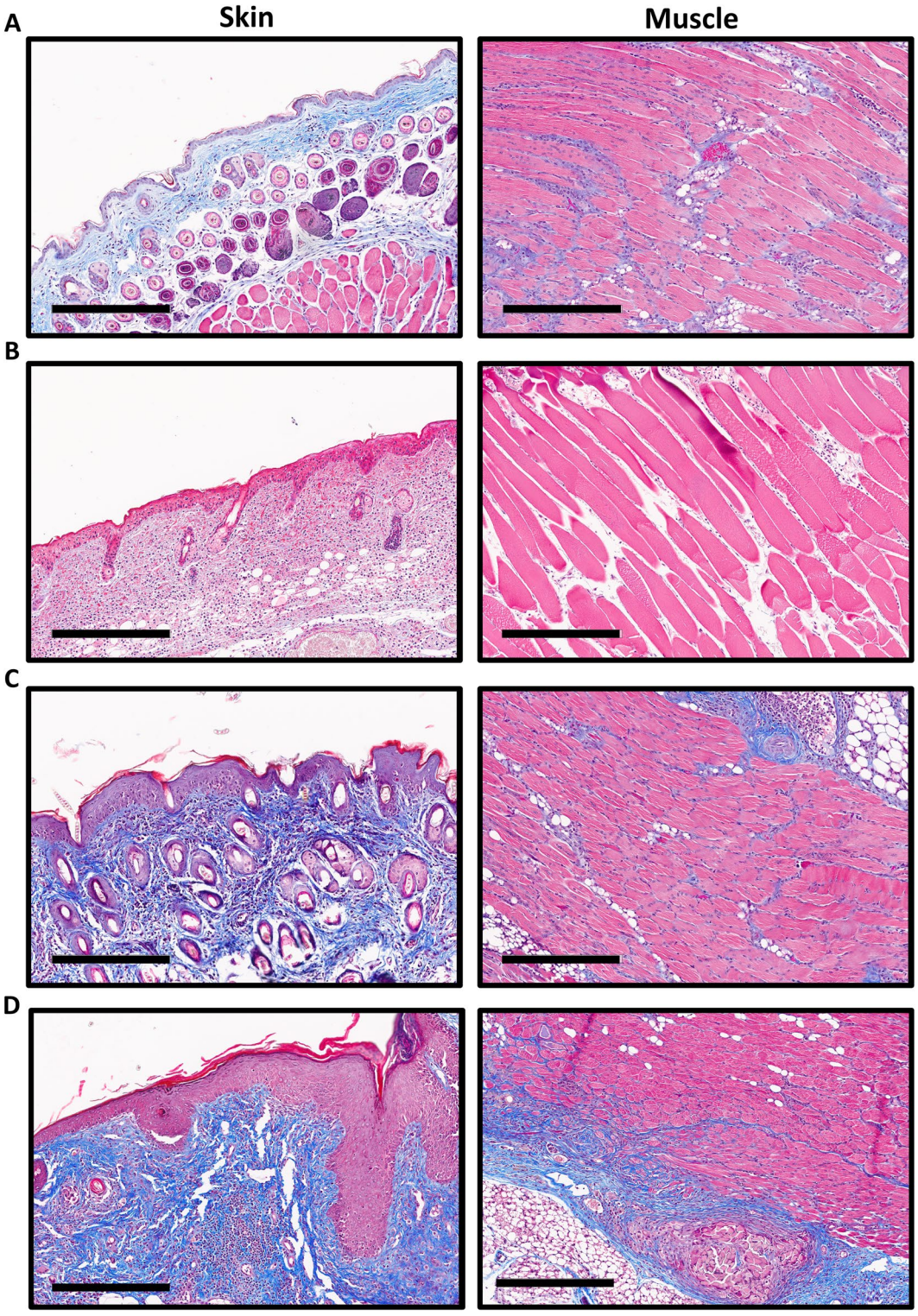

Fig. 6. Representative findings of trichrome stain in the skin and muscle after VCA. **A**, Syngeneic graft. **B**, Acute rejection graft. **C**, Chronic KO rejection graft. **D**, Chronic BM12 rejection graft. Scale bar; 300 μm.

B cell infiltration in the dermis of transplanted grafts was quantified by IHC. While there was no statistical difference between the syngeneic and acute rejection groups, significantly greater B cell infiltration was found in the chronic KO rejection group (Fig. 8). However, this finding was not observed in the chronic BM12 group (Fig. 8).

Multiple conventional immunosuppressants are routinely administered to VCA recipients. Therefore, we evaluated whether our models exhibited features of chronic rejection under treatment with tacrolimus, a widely

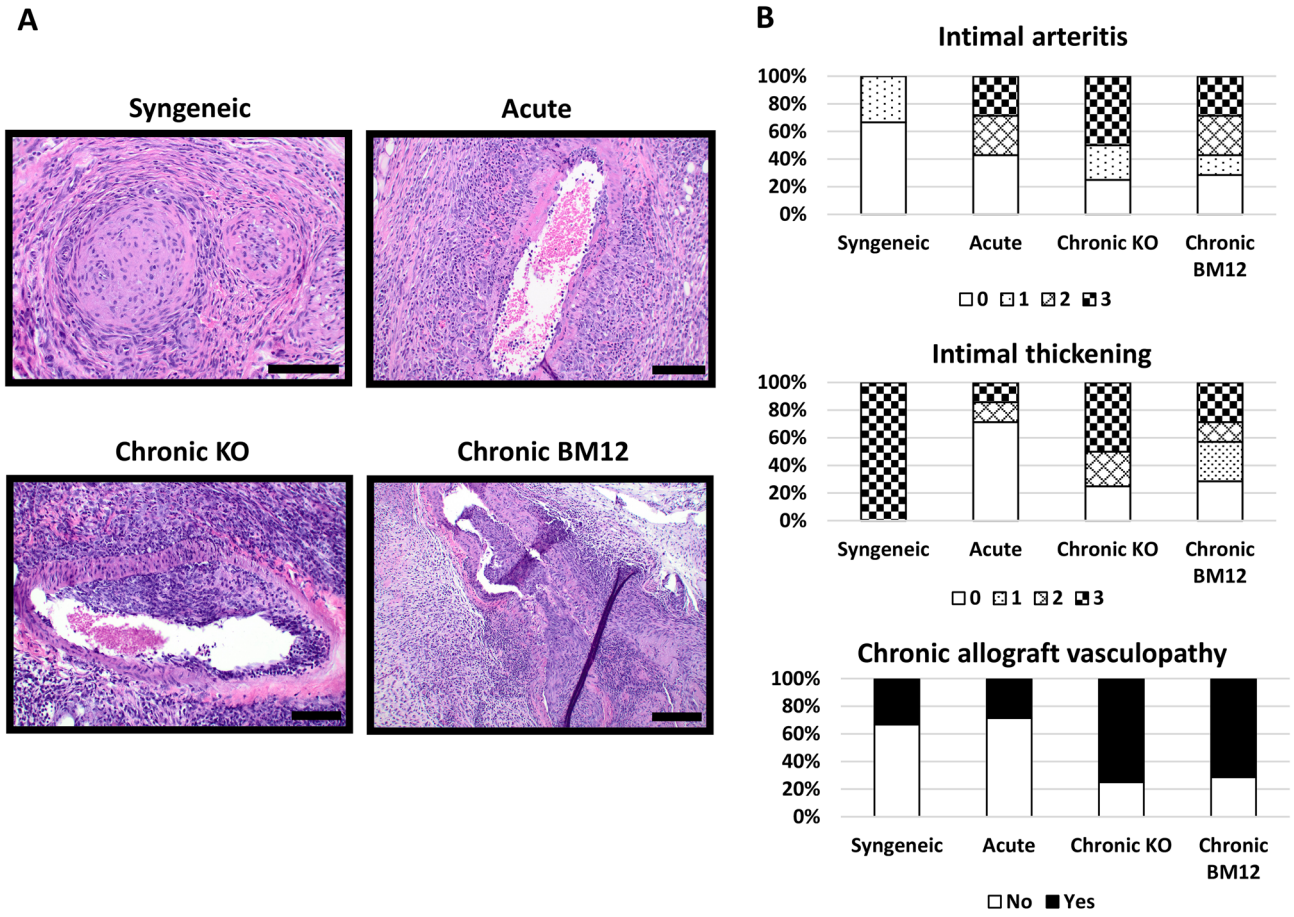

Fig. 7. Evaluation of chronic allograft vasculopathy (CAV). CAV was defined as the simultaneous occurrence of intimal thickening and endarteritis. **A**, H&E-stained image of arteries from different rejection models. Scale bar; 100 µm in syngeneic, acute, and chronic KO images, 200 µm in the chronic BM12 image. **B**, Stacked column graphs of intimal arteritis (mononuclear cells underneath arterial endothelium; 0; none, 1; < 25%, 2; > 25%, 3; transmural involvement, intimal thickening (0; none, 1; < 25%, 2; 25–50%, 3; > 50%), and CAV. Pooled data from 3 independent experiments. Syngeneic; $n = 3$, acute; $n = 7$, chronic KO; $n = 4$, and chronic BM12; $n = 7$.

used immunosuppressive agent in solid organ transplantation. No overt signs of gross rejection were observed for up to 2 weeks in the chronic KO model and 6 weeks in the bm12 model (Fig. 9A). Key histopathologic features of chronic rejection in the skin and vasculature were assessed using H&E staining (Fig. 9B). Most grafts exhibited adnexal atrophy, dermal fibrosis, and increased infiltration of dermal mast cells (Fig. 9C). Notably, one graft demonstrated concurrent intimal arteritis and vascular intimal thickening despite tacrolimus treatment (Fig. 9D). Flow cytometric analysis revealed no statistically significant difference in the total B cell population between tacrolimus-treated groups and untreated chronic models (gray; previously presented in Fig. 2) (Fig. 10A). However, plasma cell populations in the BM were effectively suppressed under tacrolimus, while a significant increase in activated B cell populations was observed in the spleen compared to untreated chronic models (Fig. 10B). Additionally, tacrolimus treatment led to a reduction in the proportion of $CD4^+$ EM T cells (Fig. 10C).

Discussion

Differentiating between acute and chronic rejection responses after VCA is challenging due to overlapping immune mechanisms, similar clinical manifestations, histopathological similarities, and the gradual progression from acute to chronic rejection. A reliable chronic VCA rejection model is vital for advancing transplant science, optimizing clinical outcomes, and ensuring that VCA remains a viable reconstructive option. To address this, the authors have introduced two distinct chronic rejection models based on differences in MHC compatibility between donors and recipients. Total MHC mismatch model was used with BALB/c (MHC I/II d) and C57BL/6 CD8 KO (MHC I/II b) strains as a donor and a recipient respectively for the chronic KO rejection model. For the chronic BM12 rejection model, single MHC disparity model was designed using B6(C)-H2-$Ab1^{bm12}$/KhEgJ donors and C57BL/6 CD8 KO (MHC I/II b) recipients. The B6(C)-H2-$Ab1^{bm12}$/KhEgJ mouse strain, commonly referred to as bm12, is a valuable model for studying chronic rejection in transplantation research. This strain carries a specific mutation in the MHC class II molecule ($I\text{-}A^{bm12}$), differing from the standard C57BL/6 (B6)

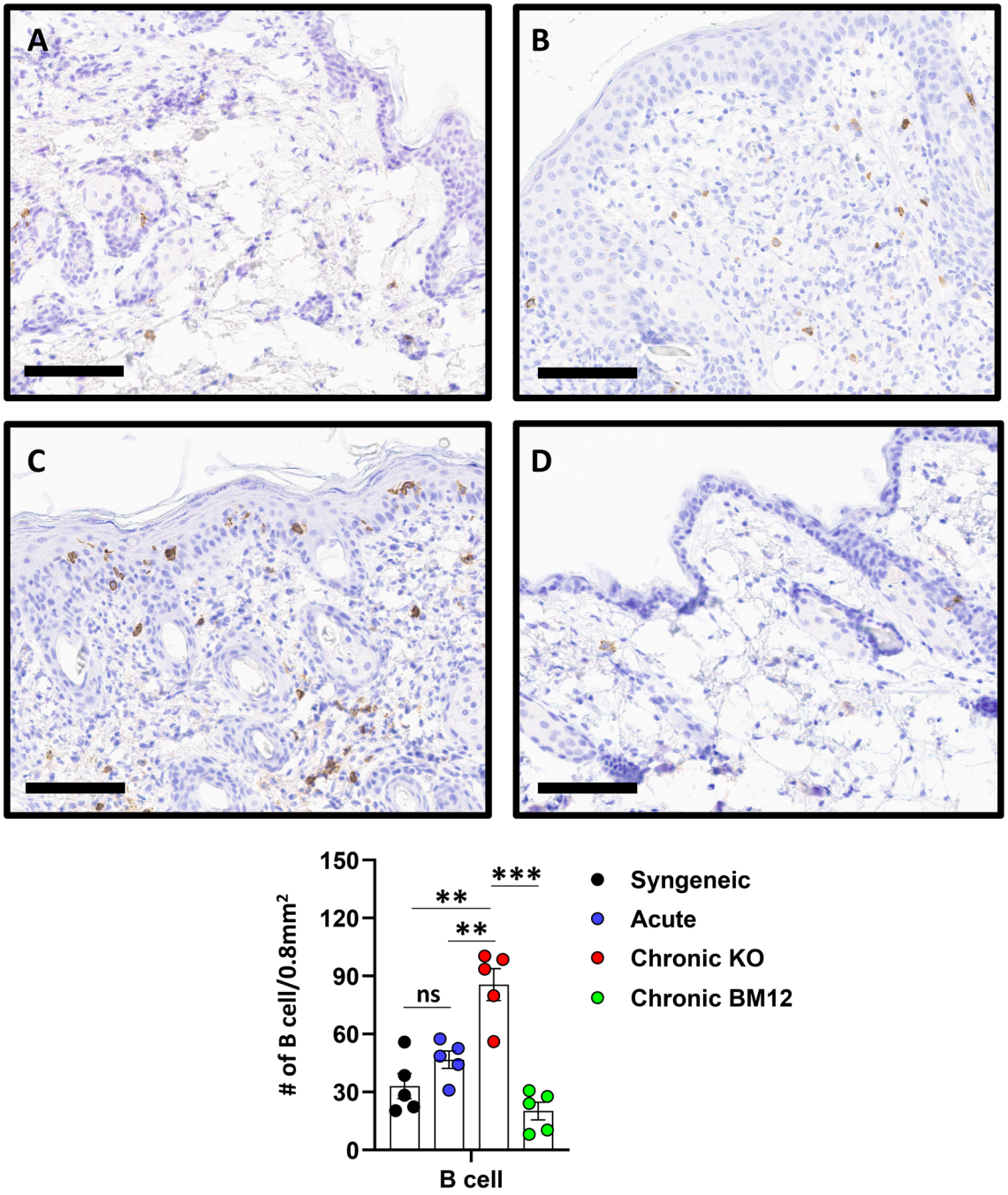

Fig. 8. Increased B cell infiltration in the grafts undergoing chronic rejection. Immunohistochemistry was performed with B220 antibody with grafts 4, 1, 2, and 6 weeks after VCA for the syngeneic, acute, chronic KO, and chronic BM12 rejection groups respectively. Positive cells with the antibody were counted by Image J program. Scale bar; 100 μm. Pooled data from 3 independent experiments. Over 4 fields from $n = 5$/group, ns; not significant, $^{**}P < 0.01$ by Student's t test, error bar; standard error of the mean.

mice by three amino acid substitutions[31]. This minor difference leads to MHC class II disparity when bm12 tissues are transplanted into B6 recipients, making it a useful model for studying the immunological and pathological processes underlying chronic rejection, as well as for testing potential therapeutic interventions[32,33]. We used the CD8 KO strain for recipients, because the deletion of $CD8^+$ T cells skew the immune response toward chronic rejection by shifting the balance toward $CD4^+$ T cell-driven humoral immunity and B cell activation, resulting in enhanced alloantibody production and antibody-mediated graft injury. A period of 14 days may initially appear to reflect rapid immune responses resembling T cell-mediated acute rejection in the chronic KO rejection model; however, this response was driven predominantly by significant B-cell infiltration into the transplanted grafts and an associated increase in DSA. The duration of gross rejection appearance in chronic BM12 recipients was

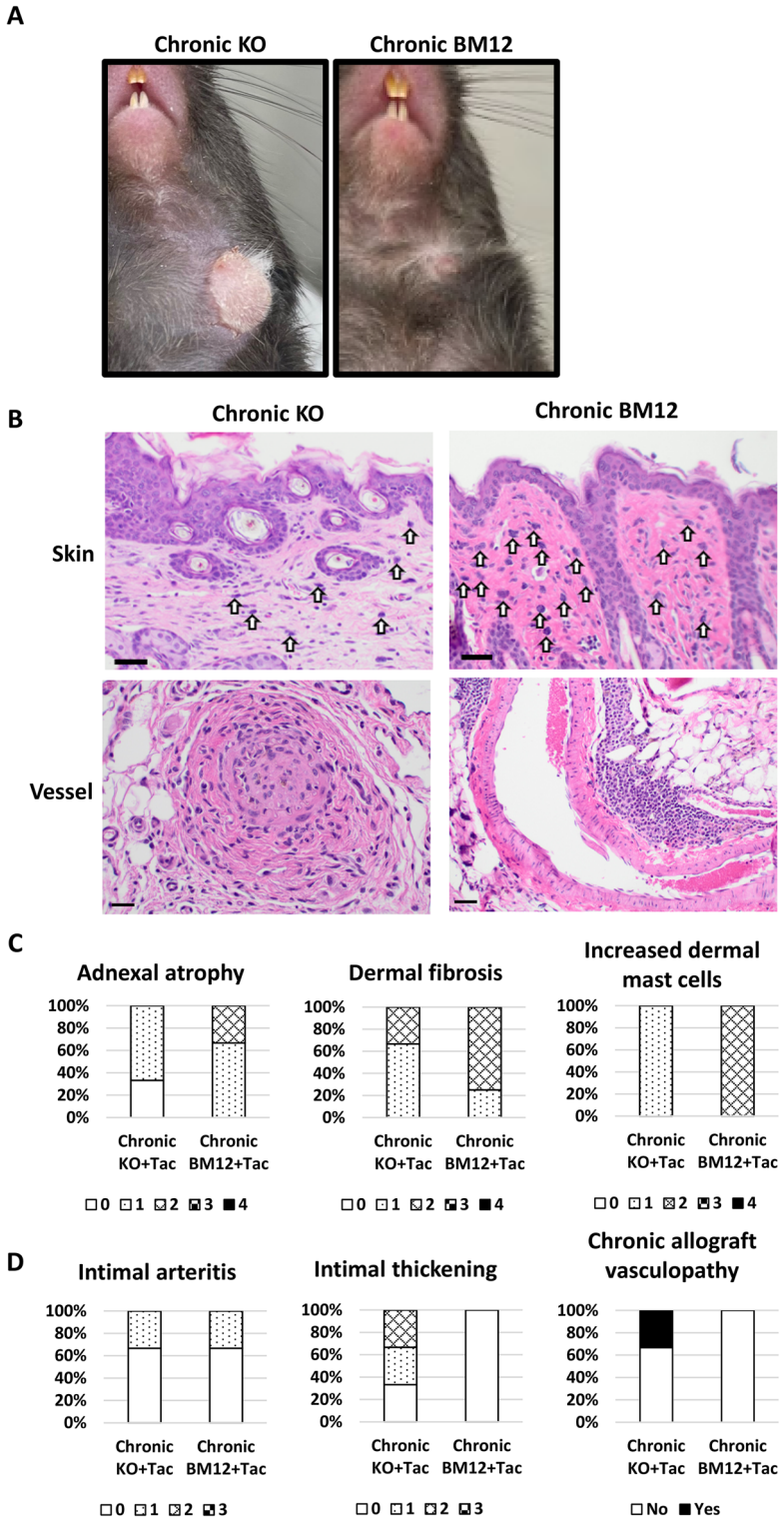

Fig. 9. Chronic rejection features following VCA under conventional immunosuppression. **A**, Representative gross findings 2 weeks and 6 weeks after chronic KO and BM12 VCA respectively. **B**, H&E-stained images of skin and vessels from chronic rejection models after using low-dose of tacrolimus. Scale bar; 20 μm, arrows; mast cell. **C**, Histopathological scores of the transplanted grafts. Stacked column graph of adnexal atrophy, dermal fibrosis, and mast cell counts in the dermis, respectively (0; none, 1; minimal, 2; mild, 3; moderate, 4; severe). **D**, Stacked column graphs of intimal arteritis (mononuclear cells underneath arterial endothelium; 0; none, 1; < 25%, 2; > 25%, 3; transmural involvement, intimal thickening (0; none, 1; < 25%, 2; 25–50%, 3; > 50%), and CAV. Data represent one independent experiment, $n = 3$ per group. Tac; low-dose tacrolimus.

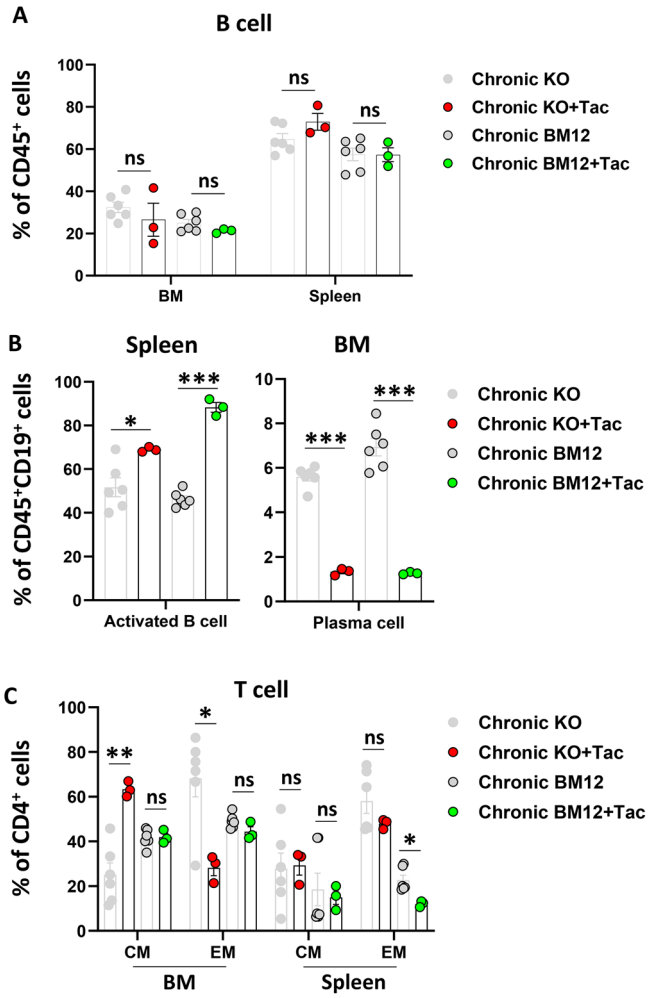

Fig. 10. Chronic rejection immune responses with low-dose of tacrolimus usage after VCA. Flow cytometric analysis of immune cell populations following VCA under low-dose tacrolimus. **A**, The composition of B cell population ($CD45^+CD3^-B220^+$) was analyzed in the BM and spleen at week 2 for the chronic KO, and at week 6 for the chronic BM12 rejection model after VCA. And activated B cell ($CD45^+CD3^-B220^+CD19^+$MHC II^+CD138^-) and plasma cell ($CD45^+CD3^-B220^+CD19^+$MHC II^+CD138^+) were analyzed in the spleen and BM respectively. **B**, The compositions of CD4 and CD8 T cell populations were investigated in the BM and spleen under different settings. **C**, CD4 T cells were subclassified depending on the status of CD44 and CD62L positivity such as central memory (CM; $CD44^+CD62L^+$) and effector memory (EM; $CD44^+CD62L^-$) in the BM and spleen. Comparisons were made between the tacrolimus untreated (gray; data previously shown in Fig. 2) and treated chronic models. Data represent one independent experiment, $n = 3$ per group, ns; not significant, $^*P < 0.05$, $^{**}P < 0.01$, and $^{***}P < 0.001$ by Student's t test, error bar; standard error of the mean. Tac; low-dose tacrolimus.

significantly longer than that in chronic KO recipients. The recipient mice were injected with anti-mouse CD4 Ab to transiently deplete CD4 T cells to stabilize the transplanted graft (i.e., to lessen immediate inflammatory responses induced by surgery and remove the T-cell help required for B-cell activation and antibody production) in the early post-transplant phase. This additional manipulation mimicked the situation in which a VCA appears to become established and then anti-graft antibodies appear later and lead to antibody mediated rejection (AMR) after initial graft success. CD4 EM T cells play a crucial role in activating B cells as well as a distinct migratory capacity compared to other memory T cell subsets because they possess chemokine receptors and adhesion molecules that enable them to migrate to peripheral tissues and inflammatory sites where they may encounter antigen re-exposure[34,35]. The chronic BM12 recipients exhibited significantly larger populations of CD4 T cells in the BM and spleen compared to the chronic KO recipients. This difference is attributed to the timing of the last anti-CD4 Ab injection, which occurred 12 days prior to data analysis in the chronic KO model, whereas in the chronic BM12 model, data were analyzed 40 days after the last injection since the chronic BM12 recipients maintained the gross integrity of their graft.

Activated B and plasma cells play a key role in the long-term detrimental effect of alloimmune-mediated injury. In transplantation, these cells can produce significant amounts of DSA[36]. These antibodies promote chronic rejection by activating complement resulting in vascular injury and allograft loss. The proposed

chronic models induced significantly greater activated B and plasma cell populations in the spleen and BM compared to the syngeneic and acute rejection settings. DSA and C4 d are considered as markers of AMR after organ transplantation[37,38]. DSA such as IgG and IgM are typically formed when the recipient's immune system encounters antigens from the donor organ. Monitoring IgG levels is especially crucial for detecting and managing AMR post-transplantation[39,40]. For this reason, we focused on measuring the levels of IgG. The amount of IgG was significantly more in the chronic rejection recipients than the acute and syngeneic recipients meaning the rejection responses in the chronic models were mediated with DSA production. Detection of C4 d deposition in the transplanted grafts, particularly in the microvasculature, can indicate ongoing complement activation and immune-mediated damage[37,38]. Unfortunately, the authors were not able to demonstrate the same levels of techniques and results using C4 d antibody in the previous publication[41] (*i.e.,* positive control samples revealed negative finding with the C4 d antibodies), instead complementary C4 d ELISA was performed to detect circulation C4 d levels in recipients after VCA.

It is also important whether the novel chronic models present pathological features of chronic rejection. Chronic rejection often involves changes in the vasculature of the transplanted organ such as vascular narrowing due to myointimal thickening[12,24,42]. These vascular changes can impair blood flow to the transplanted tissue, leading to ischemia and tissue damage. The proposed chronic models revealed vascular remodeling such as intimal thickening with luminal reduction in conjunction with intimal arteritis in major arteries. Interestingly, significant intimal thickening was observed in the syngeneic grafts without prominent intimal arteritis. This finding may be attributed to mechanical stress and hemodynamic changes caused by the heart. The VCA grafts were directly exposed to relatively high blood pressure through the common carotid artery, leading to shear stress alterations and vascular remodeling[43]. Based on this, the authors defined CAV as the presence of all key features, including intimal thickening, vessel narrowing, and intimal arteritis, within a main artery. The hallmark changes of chronic allograft vasculopathy generally take longer to manifest. However, approximately 80% of chronic KO recipients exhibited allograft vasculopathy within 2 weeks under specific conditions, including a total MHC mismatch and the absence of $CD8^+$ T cells, leading to the activation of B cells and plasma cells. Under low-dose tacrolimus treatment in the proposed models, characteristic features of chronic rejection in the skin were still evident; however, the incidence of CAV was markedly reduced. Given that the skin typically exhibits early signs of rejection, it is likely that vascular changes such as intimal arteritis and thickening emerge at later time points.

Additional key histopathologic features in the chronic rejection models were fibrosis of the dermis and deeper tissues as well as loss of adnexa[12]. While fibrotic changes in syngeneic grafts are generally less common and less severe compared to allogeneic grafts, they can still occur because of surgical trauma, ischemia–reperfusion injury, and healing processes without immune rejection[44]. There was an increased presence of mast cells in the dermis of the chronic rejection models. Mast cells have been demonstrated to play important roles in transplant immunology and an increased number of mast cells have been demonstrated in local sites in human allografts of liver, kidney, and lung[45]. In our model, the increased mast cell presence in the dermis likely mediated the observed dermal fibrosis seen in the chronic rejection models[46]. However, mast cells have also been demonstrated to play immunosuppressive and tolerogenic roles in skin allografts[47], and the role of these cells in our chronic rejection models remains ambiguous at this time.

The presence and extent of B cell infiltration within the transplanted graft can have important implications for graft outcomes and mechanisms of rejection responses[48,49]. B cells may infiltrate the graft tissue as part of the alloimmune response, where they recognize donor antigens as foreign and contribute to antibody-mediated immune reactions[50]. B cells also migrate from the bone marrow to secondary lymphoid organs such as lymph nodes, spleen, and mucosal-associated lymphoid tissues. Within these lymphoid organs, B cells interact with antigens presented by antigen-presenting cells (APCs) and undergo activation, proliferation, and infiltration[51]. Therefore, B cell infiltration may lead to chronic rejection and may be a marker of the severity in chronic rejection responses. Notably, significant increases in B cell infiltration were observed exclusively in the chronic KO rejection model, without similar findings in the chronic BM12 model. The observed difference is likely due to variations in MHC mismatch severity. BALB grafts elicit a stronger allogeneic immune response, resulting in greater B cell infiltration within the graft. In contrast, the higher IgG levels detected in the chronic BM12 model suggest that B cell activation and class switching occur primarily in lymphoid organs, such as the lymph nodes or spleen, rather than within the graft itself[52].

Although anti-mouse CD4 antibodies are commonly used in immunological research to deplete $CD4^+$ T cells, the injection schedules are varied depending on the experimental design, research objectives, and the model organism being studied. The authors tested only 1 dose, 200 μg/injection, along with 1 injection schedule (2 days before VCA, on VCA, and 2 days after VCA). The rejection severity and speed may be different with different doses of anti-CD4 antibody or different injection schedules. It is also important to note that chronic rejection is characterized by a progressive decline in graft function over time. In this study, the authors utilized a heterotopic VCA model, which, as a non-functioning unit, does not allow for direct assessment of hind limb functionality. However, the functional impairment observed in the transplanted limb is primarily driven by immune rejection responses, which are likely to be comparable between heterotopic and orthotopic VCA models. Future studies will investigate the application of these findings in an orthotopic VCA model to further evaluate functional outcomes. These novel heterotopic chronic rejection models present distinct features observed in chronic rejection after VCA in patients including hair loss, graft stricture, increased production of IgG, circulating C4 d, fibrotic tissue changes, CAV, and B cell infiltration into the transplanted grafts. The described mouse models may serve as a platform for identifying novel drugs and optimal protocols for the treatment of chronic rejection responses after VCA.

Data availability

The data that support the findings of this study are available from the corresponding author upon reasonable request.

Received: 26 December 2024; Accepted: 8 May 2025
Published online: 15 May 2025

References

1. Dubernard, J. M., Owen, E. R., Lanzetta, M. & Hakim, N. What is happening with hand transplants. *Lancet* **357**, 1711–1712. https://doi.org/10.1016/S0140-6736(00)04846-7 (2001).
2. Petit, F., Minns, A. B., Dubernard, J. M., Hettiaratchy, S. & Lee, W. P. Composite tissue allotransplantation and reconstructive surgery: First clinical applications. *Ann. Surg.* **237**, 19–25. https://doi.org/10.1097/01.SLA.0000041228.23111.30 (2003).
3. Devauchelle, B. et al. First human face allograft: Early report. *Lancet* **368**, 203–209. https://doi.org/10.1016/S0140-6736(06)68935-6 (2006).
4. Siemionow, M. & Kulahci, Y. Facial transplantation. *Semin. Plast. Surg.* **21**, 259–268. https://doi.org/10.1055/s-2007-991196 (2007).
5. Kaufman, C. L. et al. Current Status of Vascularized Composite Allotransplantation. *Am. Surg.* **85**, 631–637 (2019).
6. Haug, V. et al. The Evolving Clinical Presentation of Acute Rejection in Facial Transplantation. *JAMA Facial Plast. Surg.* **21**, 278–285. https://doi.org/10.1001/jamafacial.2019.0076 (2019).
7. Diep, G. K. et al. The 2020 Facial Transplantation Update: A 15-Year Compendium. *Plast. Reconstr. Surg. Glob. Open* **9**, e3586. https://doi.org/10.1097/gox.0000000000003586 (2021).
8. Kueckelhaus, M. et al. Vascularized composite allotransplantation: Current standards and novel approaches to prevent acute rejection and chronic allograft deterioration. *Transpl. Int.* **29**, 655–662. https://doi.org/10.1111/tri.12652 (2016).
9. Kanitakis, J. et al. Chronic Rejection in Human Vascularized Composite Allotransplantation (Hand and Face Recipients): An Update. *Transplantation* **100**, 2053–2061. https://doi.org/10.1097/tp.0000000000001248 (2016).
10. Benichou, G. et al. Immune recognition and rejection of allogeneic skin grafts. *Immunotherapy* **3**, 757–770. https://doi.org/10.2217/imt.11.2 (2011).
11. Etra, J. W., Raimondi, G. & Brandacher, G. Mechanisms of rejection in vascular composite allotransplantation. *Curr. Opin. Organ. Transplant* **23**, 28–33. https://doi.org/10.1097/MOT.0000000000000490 (2018).
12. Kaufman, C. L. et al. Defining chronic rejection in vascularized composite allotransplantation-The American Society of Reconstructive Transplantation and International Society of Vascularized Composite Allotransplantation chronic rejection working group: 2018 American Society of Reconstructive Transplantation meeting report and white paper Research goals in defining chronic rejection in vascularized composite allotransplantation. *SAGE Open Med.* **8**, 2050312120940421. https://doi.org/10.1177/2050312120940421 (2020).
13. Merola, J., Jane-Wit, D. D. & Pober, J. S. Recent advances in allograft vasculopathy. *Curr. Opin. Organ Transplant* **22**, 1–7. https://doi.org/10.1097/MOT.0000000000000370 (2017).
14. Kollar, B. et al. The Significance of Vascular Alterations in Acute and Chronic Rejection for Vascularized Composite Allotransplantation. *J. Vasc. Res.* **56**, 163–180. https://doi.org/10.1159/000500958 (2019).
15. Matar, A. J., Crepeau, R. L., Mundinger, G. S., Cetrulo, C. L. Jr. & Torabi, R. Large Animal Models of Vascularized Composite Allotransplantation: A Review of Immune Strategies to Improve Allograft Outcomes. *Front. Immunol.* **12**, 664577. https://doi.org/10.3389/fimmu.2021.664577 (2021).
16. Safi, A. F. et al. Local immunosuppression in vascularized composite allotransplantation (VCA): A systematic review. *J. Plast. Reconstr. Aesthet. Surg.* **74**, 327–335. https://doi.org/10.1016/j.bjps.2020.10.003 (2021).
17. Kaufman, C. L. et al. The role of B cell immunity in VCA graft rejection and acceptance. *Hum. Immunol.* **80**, 385–392. https://doi.org/10.1016/j.humimm.2019.03.002 (2019).
18. Unadkat, J. V. et al. Composite tissue vasculopathy and degeneration following multiple episodes of acute rejection in reconstructive transplantation. *Am. J. Transplant.* **10**, 251–261. https://doi.org/10.1111/j.1600-6143.2009.02941.x (2010).
19. Puscz, F. et al. A chronic rejection model and potential biomarkers for vascularized composite allotransplantation. *PLoS ONE* **15**, e0235266. https://doi.org/10.1371/journal.pone.0235266 (2020).
20. Kim, M., Fisher, D. T., Powers, C. A., Repasky, E. A. & Skitzki, J. J. Improved Cuff Technique and Intraoperative Detection of Vascular Complications for Hind Limb Transplantation in Mice. *Transplant. Direct* **4**, e345. https://doi.org/10.1097/txd.0000000000000756 (2018).
21. Kim, M. et al. Manipulating adrenergic stress receptor signalling to enhance immunosuppression and prolong survival of vascularized composite tissue transplants. *Clin. Transl. Med.* **12**, e996. https://doi.org/10.1002/ctm2.996 (2022).
22. Naesens, M. et al. The Banff 2022 Kidney Meeting Report: Reappraisal of microvascular inflammation and the role of biopsy-based transcript diagnostics. *Am. J. Transplant.* **24**, 338–349. https://doi.org/10.1016/j.ajt.2023.10.016 (2024).
23. Rosales, I. A. et al. Systematic pathological component scores for skin-containing vascularized composite allografts. *Vasc. Compos. Allotransplant.* **3**, 62–74 (2016).
24. Cendales, L. C. et al. Banff 2022 Vascularized Composite Allotransplantation Meeting Report: Diagnostic criteria for vascular changes. *Am. J. Transplant.* **24**, 716–723. https://doi.org/10.1016/j.ajt.2023.12.023 (2024).
25. Liu, X. & Quan, N. Immune Cell Isolation from Mouse Femur Bone Marrow. *Bio. Protoc.* https://doi.org/10.21769/bioprotoc.1631 (2015).
26. Milek, D. et al. A Systematic Review of the Reported Complications Related to Facial and Upper Extremity Vascularized Composite Allotransplantation. *J. Surg. Res.* **281**, 164–175. https://doi.org/10.1016/j.jss.2022.08.023 (2023).
27. Wilmore, J. R., Jones, D. D. & Allman, D. Protocol for improved resolution of plasma cell subpopulations by flow cytometry. *Eur. J. Immunol.* **47**, 1386–1388. https://doi.org/10.1002/eji.201746944 (2017).
28. Yi, S. G., Gaber, A. O. & Chen, W. B-cell response in solid organ transplantation. *Front. Immunol.* **13**, 895157. https://doi.org/10.3389/fimmu.2022.895157 (2022).
29. Kloc, M. & Ghobrial, R. M. Chronic allograft rejection: A significant hurdle to transplant success. *Burns Trauma* **2**, 3–10. https://doi.org/10.4103/2321-3868.121646 (2014).
30. Mehra, M. R. et al. International Society for Heart and Lung Transplantation working formulation of a standardized nomenclature for cardiac allograft vasculopathy-2010. *J. Heart Lung Transplant.* **29**, 717–727. https://doi.org/10.1016/j.healun.2010.05.017 (2010).
31. Oshima, M. & Atassi, M. Z. Effect of amino acid substitutions within the region 62–76 of I-A beta b on binding with and antigen presentation of Torpedo acetylcholine receptor alpha-chain peptide 146–162. *J. Immunol.* **154**, 5245–5254 (1995).
32. Yang, J. et al. Paradoxical functions of B7: CD28 costimulation in a MHC class II-mismatched cardiac transplant model. *Am. J. Transplant.* **9**, 2837–2844. https://doi.org/10.1111/j.1600-6143.2009.02839.x (2009).
33. Harper, I. G. et al. Augmentation of Recipient Adaptive Alloimmunity by Donor Passenger Lymphocytes within the Transplant. *Cell Rep.* **15**, 1214–1227. https://doi.org/10.1016/j.celrep.2016.04.009 (2016).
34. Gray, J. I., Westerhof, L. M. & MacLeod, M. K. L. The roles of resident, central and effector memory CD4 T-cells in protective immunity following infection or vaccination. *Immunology* **154**, 574–581. https://doi.org/10.1111/imm.12929 (2018).

35. Raphael, I., Joern, R. R. & Forsthuber, T. G. Memory CD4(+) T Cells in Immunity and Autoimmune Diseases. *Cells* https://doi.org/10.3390/cells9030531 (2020).
36. Chong, A. S. Mechanisms of organ transplant injury mediated by B cells and antibodies: Implications for antibody-mediated rejection. *Am. J. Transplant.* **20**(Suppl 4), 23–32. https://doi.org/10.1111/ajt.15844 (2020).
37. Garces, J. C. et al. Antibody-Mediated Rejection: A Review. *Ochsner. J.* **17**, 46–55 (2017).
38. Valenzuela, N. M. & Reed, E. F. Antibody-mediated rejection across solid organ transplants: manifestations, mechanisms, and therapies. *J. Clin. Invest.* **127**, 2492–2504. https://doi.org/10.1172/JCI90597 (2017).
39. Jordan, S. C., Lorant, T. & Choi, J. IgG Endopeptidase in Highly Sensitized Patients Undergoing Transplantation. *N. Engl. J. Med.* **377**, 1693–1694. https://doi.org/10.1056/NEJMc1711335 (2017).
40. Kobashigawa, J. et al. The management of antibodies in heart transplantation: An ISHLT consensus document. *J. Heart. Lung. Transplant* **37**, 537–547. https://doi.org/10.1016/j.healun.2018.01.1291 (2018).
41. Yang, X. et al. C4d as a Screening Tool and an Independent Predictor of Clinical Outcomes in Lupus Nephritis and IgA Nephropathy. *Front. Med. (Lausanne)* https://doi.org/10.3389/fmed.2022.832998 (2022).
42. Mundinger, G. S. et al. Histopathology of chronic rejection in a nonhuman primate model of vascularized composite allotransplantation. *Transplantation* **95**, 1204–1210. https://doi.org/10.1097/TP.0b013e31828d1528 (2013).
43. Brown, I. A. M. et al. Vascular Smooth Muscle Remodeling in Conductive and Resistance Arteries in Hypertension. *Arterioscler. Thromb. Vasc. Biol.* **38**, 1969–1985. https://doi.org/10.1161/ATVBAHA.118.311229 (2018).
44. Chullo, G. et al. Focusing on Ischemic Reperfusion Injury in the New Era of Dynamic Machine Perfusion in Liver Transplantation. *Int. J. Mol. Sci.* https://doi.org/10.3390/ijms25021117 (2024).
45. Morita, H., Saito, H., Matsumoto, K. & Nakae, S. Regulatory roles of mast cells in immune responses. *Semin. Immunopathol.* **38**, 623–629. https://doi.org/10.1007/s00281-016-0566-0 (2016).
46. Strattan, E. et al. Mast Cells Are Mediators of Fibrosis and Effector Cell Recruitment in Dermal Chronic Graft-vs.-Host Disease. *Front. Immunol.* **10**, 2470. https://doi.org/10.3389/fimmu.2019.02470 (2019).
47. Komi, E. A. D. & Ribatti, D. Mast cell-mediated mechanistic pathways in organ transplantation. *Eur. J. Pharmacol.* **857**, 172458. https://doi.org/10.1016/j.ejphar.2019.172458 (2019).
48. Ohm, B. & Jungraithmayr, W. B Cell Immunity in Lung Transplant Rejection - Effector Mechanisms and Therapeutic Implications. *Front. Immunol.* **13**, 845867. https://doi.org/10.3389/fimmu.2022.845867 (2022).
49. Zhang, H. et al. Transcriptionally Distinct B Cells Infiltrate Allografts After Kidney Transplantation. *Transplantation* **107**, e47–e57. https://doi.org/10.1097/TP.0000000000004398 (2023).
50. Schmitz, R. et al. B cells in transplant tolerance and rejection: friends or foes?. *Transplant Int.* **33**, 30–40. https://doi.org/10.1111/tri.13549 (2020).
51. Rastogi, I. et al. Role of B cells as antigen presenting cells. *Front. Immunol.* **13**, 954936. https://doi.org/10.3389/fimmu.2022.954936 (2022).
52. Karahan, G. E., Claas, F. H. & Heidt, S. B Cell Immunity in Solid Organ Transplantation. *Front. Immunol.* **7**, 686. https://doi.org/10.3389/fimmu.2016.00686 (2016).

Author contributions

Participated in research design: M.K. and E.A.R. Participated in the writing of the paper: M.K., E.M., and D.T.F. Participated in data acquisition: M.K., E.K., and D.T.F. Participated in data analysis: M.K., E.M., P.N.B., H.Y., U.S., J.J.S., C.L.C., and D.T.F. Participated in data interpretation: M.K., E.M., D.T.F, P.N.B., H.Y., U.S., J.J.S., P.K., M.S., C.L.C., and E.A.R. Participated in critical revision: M.K., J.J.S., and E.A.R. All authors discussed results and commented on the manuscript. All authors reviewed the manuscript.

Funding

This research was supported by HT9425-23–1-0529 from DoD, Roswell Park Alliance Foundation, and Cancer Center Support Grant P30 CA06156.

Declarations

Competing interests

The authors declare no competing interests.

Additional information

Correspondence and requests for materials should be addressed to M.K.

Reprints and permissions information is available at www.nature.com/reprints.

Publisher's note Springer Nature remains neutral with regard to jurisdictional claims in published maps and institutional affiliations.